Developmental Cell
Short Article

Unilateral Dampening of Bmp Activity by Nodal Generates Cardiac Left-Right Asymmetry

Justus Veerkamp,[1] Franziska Rudolph,[1] Zoltan Cseresnyes,[2,3] Florian Priller,[1] Cécile Otten,[1] Marc Renz,[1] Liliana Schaefer,[4] and Salim Abdelilah-Seyfried[1,*]
[1]Cardiovascular Department
[2]Confocal and 2-Photon Microscopy Core Facility
Max Delbrück Center for Molecular Medicine, Robert-Rössle-Straße 10, 13125 Berlin, Germany
[3]German Rheumatism Research Center (DRFZ), a Leibniz Institute, Charitéplatz 1, 10117 Berlin, Germany
[4]Institute for General Pharmacology and Toxicology, Goethe University, Theodor-Stern Kai 7, 60590 Frankfurt/Main, Germany
*Correspondence: seyfried@mdc-berlin.de
http://dx.doi.org/10.1016/j.devcel.2013.01.026

SUMMARY

Signaling by Nodal and Bmp is essential for cardiac laterality. How activities of these pathways translate into left-right asymmetric organ morphogenesis is largely unknown. We show that, in zebrafish, Nodal locally reduces Bmp activity on the left side of the cardiac field. This effect is mediated by the extracellular matrix enzyme Hyaluronan synthase 2, expression of which is induced by Nodal. Unilateral reduction of Bmp signaling results in lower expression of nonmuscle myosin II and higher cell motility on the left, driving asymmetric displacement of the entire cardiac field. In silico modeling shows that left-right differences in cell motility are sufficient to induce a robust, directional migration of cardiac tissue. Thus, the mechanism underlying the formation of cardiac left-right asymmetry involves Nodal modulating an antimotogenic Bmp activity.

INTRODUCTION

Most internal organs show a distinct laterality with respect to the left-right (L/R) body axis as a result of asymmetric morphogenesis. L/R asymmetry depends on the evolutionarily conserved Nodal signaling pathway (Chen et al., 2010; Schier, 2009) and other morphogenetic growth factors, including Bmp, which is required for cardiac laterality (Breckenridge et al., 2001; Chocron et al., 2007; Schilling et al., 1999; Smith et al., 2008; Zhang and Bradley, 1996). In zebrafish, cardiac asymmetry is initiated by a leftward extension of the cardiac tube in a process referred to as cardiac jogging (Chen et al., 1997), which is driven by the active migration of cardiac progenitor cells (Baker et al., 2008; de Campos-Baptista et al., 2008; Rohr et al., 2008; Smith et al., 2008). The initiation of cardiac L/R asymmetry requires Southpaw (Spaw)/Nodal-related-3, a Nodal ligand that is expressed within the left lateral plate mesoderm (Long et al., 2003); Hyaluronan synthase 2 (Has2), which is an extracellular matrix (ECM)-modifying enzyme dependent on Spaw (Smith et al., 2008); and Bmps that are expressed within the cardiac cone (Chen et al., 1997; Schilling et al., 1999). Previous observations suggested a crosstalk whereby Nodal induced stronger left-sided Bmp expression within the heart (Chen et al., 1997; Chocron et al., 2007). According to this model, elevated Bmp levels would then enhance myocardial progenitor cell motility toward the left (Smith et al., 2008). However, this failed to explain the mode of interaction between Nodals and Bmp, the molecular role of Has2 in cardiac jogging, the mechanism by which an asymmetry of Bmp activity is established within the heart prior to cardiac jogging, and the means by which Bmp regulates myocardial progenitor cell motility.

In contrast to previous reports, our findings suggest that Bmp activity is dampened on the left by Nodal-Has2 and that Bmp signaling impairs the motile behavior of cardiac progenitor cells. Experimental measurements and mathematical modeling show that subtle differences in "random walk" cell motility rates on left side versus right side from the midline are sufficient to shape an organ whose asymmetry is so vital to its function.

RESULTS

Nodal Antagonizes Bmp Activity within the Heart

Prior to cardiac jogging, Bmps are strongly expressed within the heart cone (Figure 1A; see also Figure S1 available online). To elucidate the molecular crosstalk between the Nodal and Bmp pathways, we assayed Bmp signaling activity at the level of the downstream receptor-regulated- (R-) Smads-1/5/8 that are phosphorylated (pSmad-1/5/8) upon binding of Bmps to their type I and type II serine/threonine kinase receptors. Although *bmp4* expression is bilaterally symmetrical prior to cardiac jogging at 19 hr postfertilization (hpf) (Figure 1A), Bmp signaling activity is significantly lower in myocardial progenitor cells on the left side compared to those on the right side of the cardiac cone (Figures 1B and 1C). This finding seems to contradict the current model on cardiac L/R asymmetric Bmp signaling, which implies that Bmp signaling should be higher on the left (Chen et al., 1997; Smith et al., 2008). If this L/R asymmetry depends on left-sided Nodal activity, then it should be abolished upon loss of Spaw. Indeed, antisense oligonucleotide morpholino- (MO)- mediated knockdown of Spaw (Long et al., 2003) resulted in symmetrical Bmp signaling activity on both sides of the cardiac cone (Figure 1C). To verify these findings with an independent assay, we used the transgenic Bmp response element (BRE) reporter line Tg[*BRE-AAVmlp:dmKO2*]^{mw40}, which is based on a destabilized

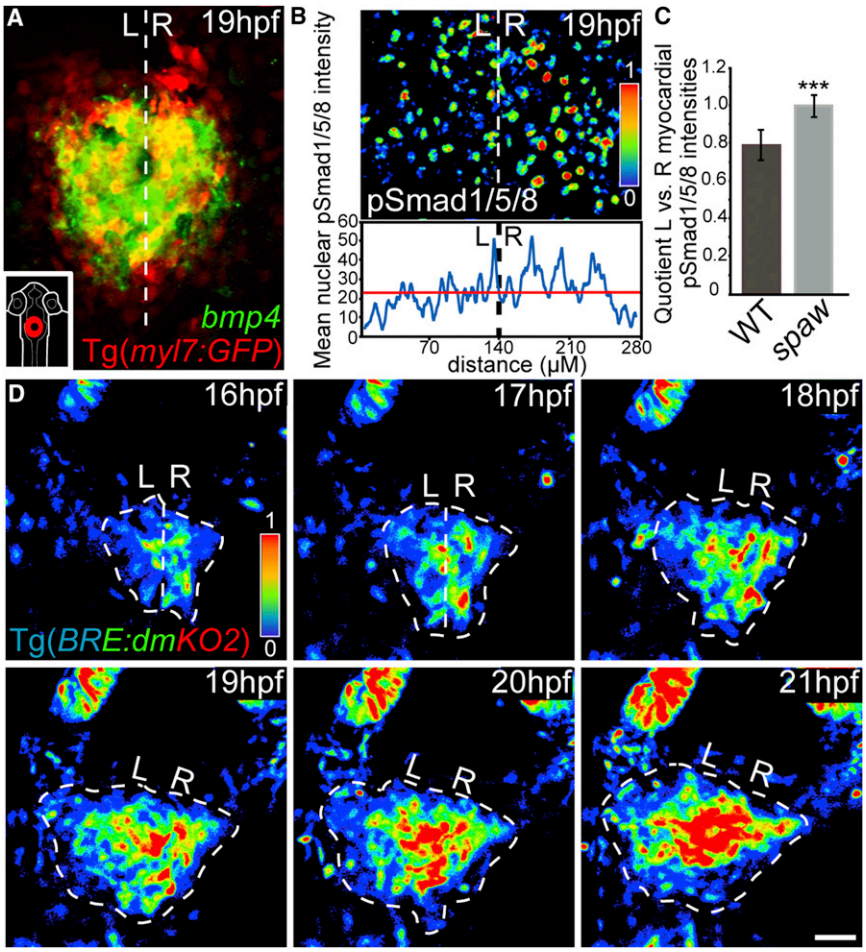

Figure 1. Bmp Signaling Is Weaker within the Left Heart Cone prior to the Appearance of Morphological Asymmetries

(A) Fluorescence two-color in situ hybridization of *bmp4* expression at the heart cone stage (false-colored image).

(B) Cardiac progenitor cells have lower nuclear pSmad-1/5/8 intensities on the left side of the heart as indicated by the color range. The mean intensity plot is a measure of the entire intensities within the field of view.

(C) The L/R asymmetry of nuclear pSmad-1/5/8 intensities is abolished in *spaw* morphant embryos at 19 hpf (mean with SD based on quantifications of eight hearts per genotype; ***$p < 0.0005$).

(D) The laterality of cardiac jogging coincides with lower intensities of Bmp signaling activity as indicated by the Bmp reporter line Tg[*BRE-AAVmlp:dmKO2*]^{mw40} (false-colored image). White dotted line indicates the embryonic midline. Scale bar, 50 μm. L, left; R, right.

See also Figures S1, S2, and Movie S1.

reporter protein that faithfully recapitulates pSmad-1/5/8-mediated activity (Collery and Link, 2011). Time-lapse analyses of cardiac cone and early cardiac jogging stages (16–21 hpf) revealed a dynamic pattern of Bmp signaling activity that is weaker on the left side prior to the first appearance of any morphological asymmetry and during the initial stages of cardiac jogging (Figure 1D; see also Movie S1) and that is symmetrical upon loss of Spaw (see also Figure S2). Together, these findings indicate that Nodal has an inhibitory effect on Bmp activity on the left side of the heart during L/R asymmetric cardiac morphogenesis.

To directly test whether Spaw antagonizes Bmp signaling activity within the heart, we misexpressed Spaw from a myocardial *myosin light chain7* (*myl7*) promoter expression construct, Tg[*myl7:spaw_IRES_CAAX-EGFP*], which was injected at the one-cell stage into the Tg[*BRE-AAVmlp:dmKO2*]^{mw40} reporter line. Subsequently, we performed time-lapse analyses of cardiac progenitor cells (Figures 2A and 2B) in preselected embryos with Spaw-expressing clones that were by chance predominantly distributed within the right cardiac field and assayed their effects on Bmp signaling activity and on cardiac laterality. In each case, right-sided Spaw-expressing clones affected cardiac laterality and resulted in a reversal of cardiac jogging (Figure 2B; see also Movie S2), unlike left-sided Spaw-expressing clones that did not impact cardiac laterality (n = 4/4 embryos). Relative quantifications of Bmp signaling activity on both sides of the cardiac cone based on the Tg[*BRE-AAVmlp:dmKO2*]^{mw40} reporter line revealed a relative inversion of Bmp signaling activity within such hearts. Thus, myocardial cells surrounding Spaw-expressing clones have a reduced Bmp signaling activity possibly due to an inhibitory non-cell-autonomous effect of Spaw on Bmp.

Together, these findings raised the possibility that Nodal may regulate cardiac laterality by dampening Bmp signaling and that Bmp activity, in turn, essentially controls cardiac laterality downstream of Nodal. If this assumption is correct, then modulating Bmp signaling activity within the cardiac cone should be sufficient to affect laterality even in the presence of normal endogenous L/R asymmetrical Nodal signaling. We tested this hypothesis by inducing either dominant-negative Bmp type II receptor a (dnBmpr2a) (Monteiro et al., 2008) or Bmp antagonist Noggin1 (Dal-Pra et al., 2006) within myocardial cell clones (Figures 2D and 2E). Consistent with the prediction that modulating Bmp signaling activity should affect laterality of the heart, we found that reduced Bmp activity inverts cardiac laterality when such clones are initially positioned on the right side of the cardiac cone at 18 hpf. That Bmp signaling is reduced was verified using the Tg[*BRE-AAVmlp:dmKO2*]^{mw40} reporter (see insets in Figures 2C–2E), which revealed that the mean intensities in dnBmpr2a- or Noggin1-misexpressing cells are lower than in their neighboring cells (ratios of mean expression intensities based on 20 misexpressing versus 20 neighboring control cells: *myl7:EGFP*/wild-type [WT] [0.99 ± 0.06 SD], *myl7:noggin1*/WT [0.31 ± 0.09 SD], and *myl7:dnbmpr2a*/WT [0.45 ± 0.02 SD]). Because these clones do not affect normal expression of the Nodal pathway genes *lefty1* (*lft1*) (Figure 2F; total of four hearts analyzed with 10 left-sided and 26 right-sided clones) or *nodal-related 2*

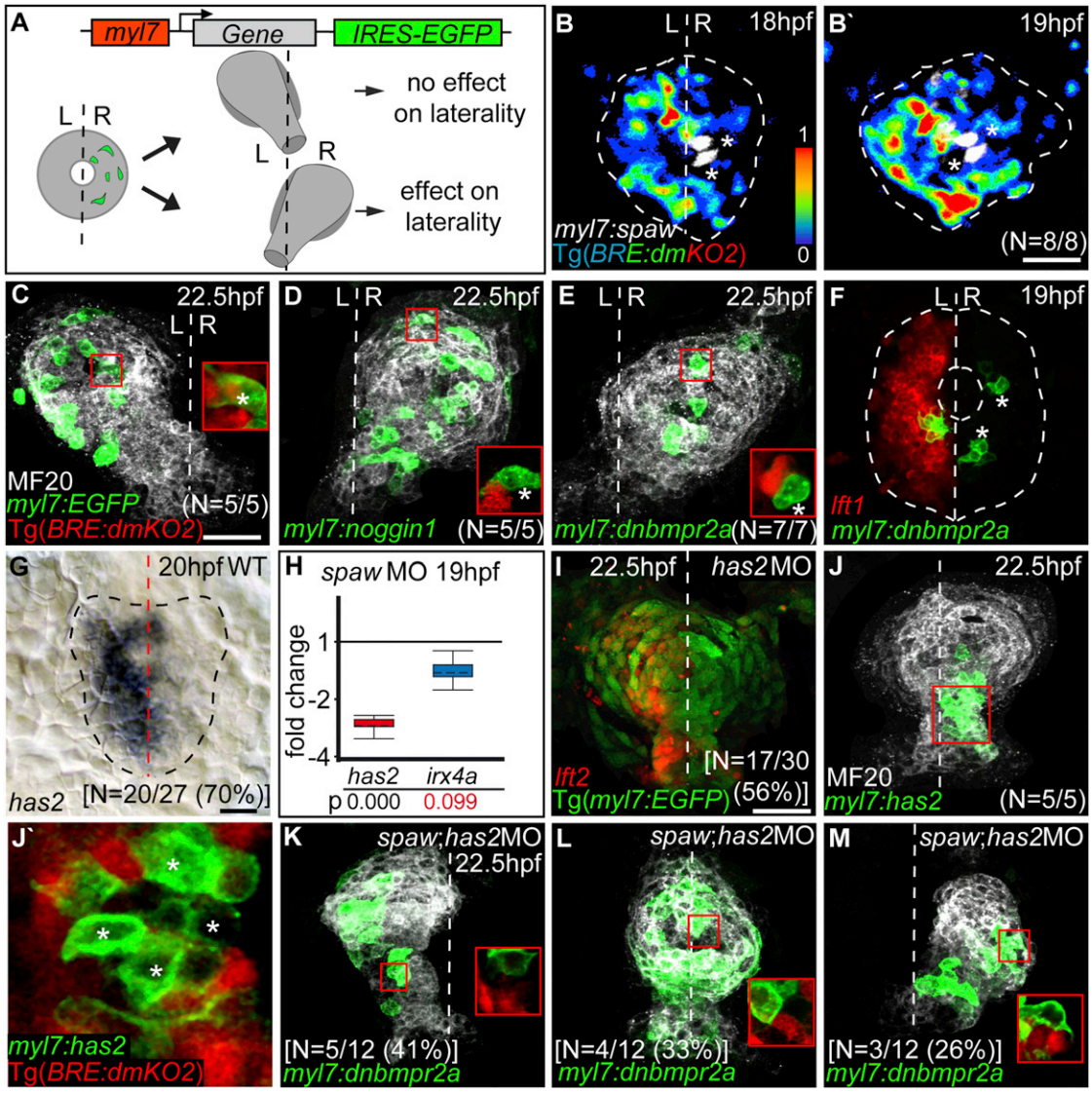

Figure 2. Tissue-Autonomous Inhibition of Bmp Activity Affects Cardiac Laterality

(A) Cardiac laterality was assayed at 22.5 hpf in embryos with predominantly right-sided myocardial cell clones at 18 hpf.

(B and B′) Spaw-expressing clones (false-colored white, indicated by asterisks) cause reversal of Bmp reporter Tg[*BRE-AAVmlp:dmKO2*]^{mw40} relative expression intensities, indicated by color range as shown for 18 hpf (B) and for 19 hpf (B'). Cardiac field is outlined by white dotted circle.

(C) Control clones expressing enhanced green fluorescent protein (EGFP) do not affect cardiac jogging. Inset shows expression of the Tg[*BRE-AAVmlp:dmKO2*]^{mw40} Bmp reporter in control clone (asterisk) and neighboring cells.

(D and E) Misexpression of the Bmp antagonist Noggin1 (D) or of dnBmpr2a (E) on the right side of the cardiac cone causes rightward cardiac jogging. Insets show specific suppression of Bmp activity within EGFP-positive misexpression clones (asterisk).

(F) Fluorescence two-color in situ hybridization reveals normal *lefty1* cardiac expression in clones expressing dnBmpr2a.

(G) L/R asymmetric expression of *has2*.

(H) Whisker box plots indicate relative expression changes of *has2* and *irx4a* based on RT-qPCR analysis of cardiac cDNA (also see Supplemental Experimental Procedures for details on the statistical analysis). Unchanged expression of the cardiac stage marker *irx4a* shows that observed changes in *has2* expression are not due to developmental delay.

(I) Fluorescence two-color in situ hybridization of a *has2* morphant with loss of cardiac laterality but correct *lefty2* expression.

(J) Clonal misexpression of Has2 on the right side of the cardiac cone affects cardiac laterality.

(J′) Bmp activity is specifically suppressed within EGFP-positive Has2-misexpression clones (asterisks) but not in neighboring WT cells.

(K–M) Cardiac laterality in *spaw;has2* double morphants that have EGFP-positive dnBmpr2a misexpression clones. Cardiac laterality at 22.5 hpf strictly corresponds to the L/R distribution of dnBmpr2a-expressing cell clones. Shown are examples for mainly left-sided (K), evenly distributed (L), or right-sided (M) dnBmpr2a-expressing cell clones. Insets show that Bmp activity is specifically suppressed within EGFP-positive misexpression clones.

L, left; R, right. Dotted line indicates the embryonic midline. Total number of embryos and percentiles indicate the occurrence of the most frequent expression patterns and phenotypes as shown. Scale bars, 50 μm.

See also Movie S2.

(*ndr2*) (total of four hearts analyzed with four left-sided and 24 right-sided clones) on either the left or right sides of the cardiac cone, Bmp-mediated reversal of cardiac laterality does not involve a reversal of Nodal expression.

The Extracellular Matrix Modulating Enzyme Hyaluronan Synthase 2 Dampens Bmp Activity

We next sought to elucidate the mechanism by which Nodal modulates Bmp signaling activity within the left cardiac cone. If Bmp indeed acts downstream of Nodal, the mechanism by which Spaw negatively modulates Bmp signaling activity should also involve Nodal targets that affect cardiac laterality. To explore this hypothesis, we focused on the Nodal target *has2*, which has an asymmetric and Spaw-dependent expression on the left side of the cardiac cone (Figures 2G and 2H) (Smith et al., 2008) and is required for both zebrafish cardiac laterality and murine cardiac morphogenesis (Camenisch et al., 2000; Smith et al., 2008). Has2 is one of three enzymes involved in the production of hyaluronic acid, a major macromolecule of the ECM. However, functional analyses of Has2 during cardiac morphogenesis are complicated by an additional and earlier role of this enzyme during gastrulation (Bakkers et al., 2004) which impacts the establishment of L/R asymmetry. Consistent with an early role of Has2 in L/R patterning, we found that cardiac laterality is affected in a majority of *has2* morphants, which frequently results in midline hearts (n = 42/72 [58.3%] of embryos). Unexpectedly, L/R patterning was not affected in 56% of *has2* morphants that have a midline heart as indicated by normal left-sided *lefty2* expression (n = 17/30 [56.7%] embryos; Figure 2I). Hence, loss of cardiac laterality in *has2* morphants frequently does not affect expression of *lefty2*, which is indicative of a role of Has2 downstream of Nodal signaling within the cardiac field. Consistent with this finding, we observed that *lefty2* expression was unaffected in *has2* morphants that showed normal cardiac laterality (data not shown). To further elucidate the potential role of Has2 for Bmp signaling activity within the cardiac field, we next used an overexpression strategy. Since high expression levels of *has2* on the left side of the cardiac cone correlate with dampened Bmp signaling activity, we expected that clonal misexpression of Has2 within myocardial cells might also reduce Bmp signaling activity. Indeed, clonal myocardial expression of Has2 results in strong dampening of Bmp activity as indicated by the Tg[*BRE-AAVmlp:dmKO2*]^{mw40} reporter (Figures 2J and 2J′; ratio of mean expression intensities based on 20 Has2-expressing versus 20 neighboring control cells: *myl7:-has2*/WT [0.38 ± 0.13 SD]). Consistent with the effects of unilaterally reduced Bmp signaling, cardiac laterality is strongly affected when Has2 misexpression clones are positioned predominantly on one side of the cardiac cone at 18 hpf (Figure 2J).

If Has2 affects cardiac laterality by dampening Bmp signaling activity, unilaterally reducing Bmp signaling activity should restore cardiac laterality even in the absence of the enzyme. To test *has2* loss-of-function conditions in such an epistasis experiment, we took advantage of the fact that its cardiac expression is strongly reduced in *spaw* morphants (Figure 2H) that otherwise develop normally because the expression of this Nodal ligand initiates after gastrula stages (Long et al., 2003). To further reduce remnant Has2 levels within the cardiac cone of *spaw* morphants, we coinjected low-dosage *has2* MO together with standard dosage *spaw* MO. Such *spaw*;*has2* double morphants are indistinguishable from *spaw* single morphants in that both undergo normal gastrulation and fail to develop cardiac laterality (n = 111/123 [90.2%]). Within double morphants, upon clonal induction of dnBmpr2a, cardiac laterality at 22.5 hpf strictly corresponded to the L/R distribution of Bmp signaling-impaired cell clones (Figures 2K–2M). In contrast, control clones exhibited no effects on cardiac laterality (n = 14/15 [93%] of *spaw;has2* double morphants with GFP-control clones lack cardiac laterality). That the loss of Has2 does not render cells irresponsive to Bmp activity is further supported by the finding that expression from the Bmp signaling reporter (see insets in Figures 2K–2M) is unaffected in *spaw*;*has2* double morphants. Therefore, Spaw-Has2-deprived cardiac progenitor cells are responsive to Bmp signaling activity. Taken together, these observations reveal that Spaw exerts an inhibitory effect on Bmp signaling activity via Has2, implying that hyaluronic acid-proteoglycans antagonize the activity of locally secreted Bmp ligands.

Bmp Exerts an Antimotogenic Effect on Cardiac Progenitor Cells via Regulation of Nonmuscle Myosin II

Cardiac progenitor cells exhibit different migration speeds during cardiac jogging (de Campos-Baptista et al., 2008; Smith et al., 2008; Rohr et al., 2008; Baker et al., 2008). We speculated that lowering Bmp activity on the left induces cardiac jogging via increased cardiac progenitor cell motility rates on that side. Indeed, live imaging with myocardial (Rohr et al., 2008) and endocardial/endothelial reporter lines (Jin et al., 2005; Lawson and Weinstein, 2002) revealed that, in the WT, between 19 and 23 hpf, cardiac progenitor cells on the left migrate with significantly higher velocities than those on the right (Figure 3A; see also Movie S3). We found that loss of Spaw abolishes the left-right bias and generally reduces cardiac progenitor cell motility (Figures 3A–3C). Consistent with an increase of Bmp signaling in *spaw* morphants, we found that an enhancement of Bmp signaling activity in Tg[*hsp70l:bmp2b*]^{fr13} transgenic embryos (Chocron et al., 2007) heat shocked briefly prior to cardiac jogging also has a strong antimotogenic effect on cardiac progenitor cells (Figures 3B and 3C; see also Movie S4).

To identify relevant Bmp-dependent cardiac effector genes, we next performed a comparative microarray expression analysis with cardiac tissue isolated from 21.5 hpf WT and Tg[*hsp70l:bmp2b*]^{fr13} embryos heat shocked at 18 hpf to induce Bmp2b expression. Many of the genes upregulated upon Bmp overactivation encode cell adhesion proteins or determinants of epithelial character (Figure 4A; for a partial list of genes upregulated upon Bmp overactivation, see also Figure S3).

Among these, the heavy polypeptide 9a (*myh9a*/*myh9l2*) subunit of nonmuscle myosin II (NMII), is positively regulated by Bmp2b and is also upregulated upon loss of Spaw (Figure 4B; see also Figure S3B). NMII is an important regulator of dynamic cellular processes including cell polarity, migration, and epithelial remodeling (Conti and Adelstein, 2008; Widmann and Dahmann, 2009; Lecuit et al., 2011). To determine the L/R distribution of NMII within the cardiac cone, we compared

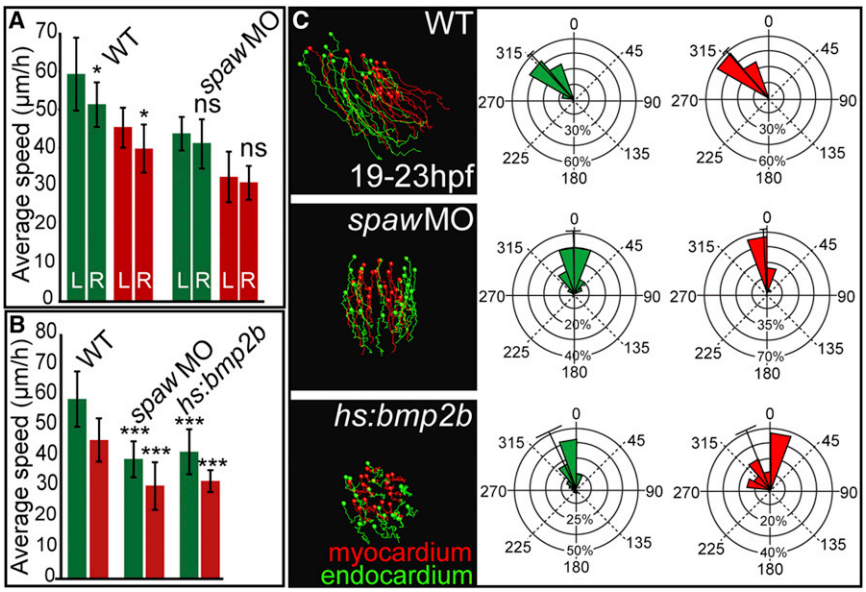

Figure 3. Nodal and Bmp Signaling Affect Cardiac Progenitor Cell Motility and Laterality

(A) Quantifications of cell motilities based on time-lapse analyses of endothelial and myocardial reporter lines between 19 and 23 hpf. In WT, endocardial (green) and myocardial (red) progenitor cell motility rates are significantly different between the left and right (mean with SD based on quantifications of at least n = 22 endocardial and n = 30 myocardial cells per genotype; *p < 0.025), whereas no significant L/R differences are observed in *spaw* morphants.

(B) Average speed measurements for *spaw* morphants or Bmp2b-overexpressing endocardial (green) and myocardial (red) progenitor cells reveal highly significant differences compared with WT (mean with SD based on quantifications of at least n = 16 endocardial cells and n = 16 myocardial cells per genotype; ***p < 0.0005).

(C) Myocardial (red) and endocardial (green) progenitor cell tracks based on live imaging. Bearing angles summarize all endocardial and myocardial cell tracks. ns, not significant.

See also Movies S3 and S4.

contralateral levels of phosphorylated myosin light chain II, which is the activated form of this motor molecule. At 20.5 hpf, increased levels of phosphorylated NMII are detectable on the right side of the cardiac cone, consistent with elevated Bmp activity on this side of the cardiac cone (Figure 4C). In comparison, phosphorylated NMII is symmetrically expressed on both sides of the cardiac cone in Tg[*hsp70l:bmp2b*]^{fr13} embryos heat shocked at 18 hpf (Figure 4D). Thus, NMII may be a player in Bmp-mediated regulation of cardiac laterality.

To functionally assess the role of NMII in this process, we clonally increased the activity of the calcium-dependent Myosin light chain kinase (MLCK), which is a major regulator of NMII function (Lecuit et al., 2011). Phosphorylation of the Myosin regulatory light chain activates NMII and promotes actin-myosin contraction (Amano et al., 1996). Myocardial clonal expression of a constitutively active form of Myosin light chain kinase (caMLCK) (Blaser et al., 2006) had a strong instructive effect on cardiac laterality. Predominantly left-sided caMLCK clones at 19 hpf correlated with a reversal of cardiac laterality or a straight midline heart tube (n = 9/9 hearts with left-sided caMLCK clones jogged to the right or straight anterior; Figure 4E). In a second experiment, we conditionally blocked NMII activity using different concentrations of the specific inhibitor Blebbistatin (Straight et al., 2003) at 18 hpf and found that heart tube elongation and motility of cardiac progenitor cells was reduced compared to WT (see also Figures S3C–S3G). In a final experiment, we compared heart tube elongation in *no tail* (*ntl*) and *spaw* morphants (Figures 4F and 4G). Loss of Ntl results in bilateral *spaw* expression domains (Long et al., 2003) and abolishes cardiac laterality. Hence, in contrast to the upregulation of *myh9l2* in *spaw* morphants, bilateral expression of Spaw in *ntl* morphants corresponded with significantly lower expression levels of *myh9l2* (Figure 4H). Consistent with a role of NMII in cardiac progenitor cell motility, heart tube elongation in these two morphants inversely correlated with expression levels of *myh9l2* (Figures 4H and 4I). Low expression levels of *myh9l2* in *ntl* morphants corresponded with an extended heart tube, whereas high levels of *myh9l2* expression in *spaw* morphants correlated with a shorter heart tube. Taken together, these findings demonstrate an important role of NMII during cardiac jogging and suggest that NMII activity on the left side of the cardiac cone is slightly lower than on the right.

Zebrafish Cardiac Jogging Can Be Modeled Based on a "Random Walk" Motility Mechanism

Our functional data implied that Nodal generates cardiac asymmetry via unilateral dampening of an antimotogenic Bmp activity. To simulate whether L/R differences in cell motility rates explain cardiac laterality, we developed a mathematical model of cardiac jogging behavior. In brief, we modeled collective tissue migration based on the assumption that cells on both sides of the midline could freely choose a random walk, but those on the left moved slightly faster (see Supplemental Experimental Procedures). Simulations using this model resulted in a robust leftward displacement of the entire coherent sheet of cells (Figure 4J; see also Figure S4A). We adjusted the model based on the finding that the expression of Nodal components strongly diminishes during cardiac jogging stages (see also Figure S4B). Therefore, Bmp activity may be only transiently affected by Nodal to initiate cardiac jogging. In our model, the collapse of left-sided Nodal (represented by a time-dependent incremental reduction in the left-sided cell motility bias) results in a rotational turning similar to the rotational motion of the cardiac tube during jogging stages (Baker et al., 2008; de Campos-Baptista et al., 2008; Smith et al., 2008).

As an experimental test of the in silico model, we analyzed cardiac jogging in embryos with a stronger left-sided reduction of Bmp signaling activity due to left-sided Noggin1

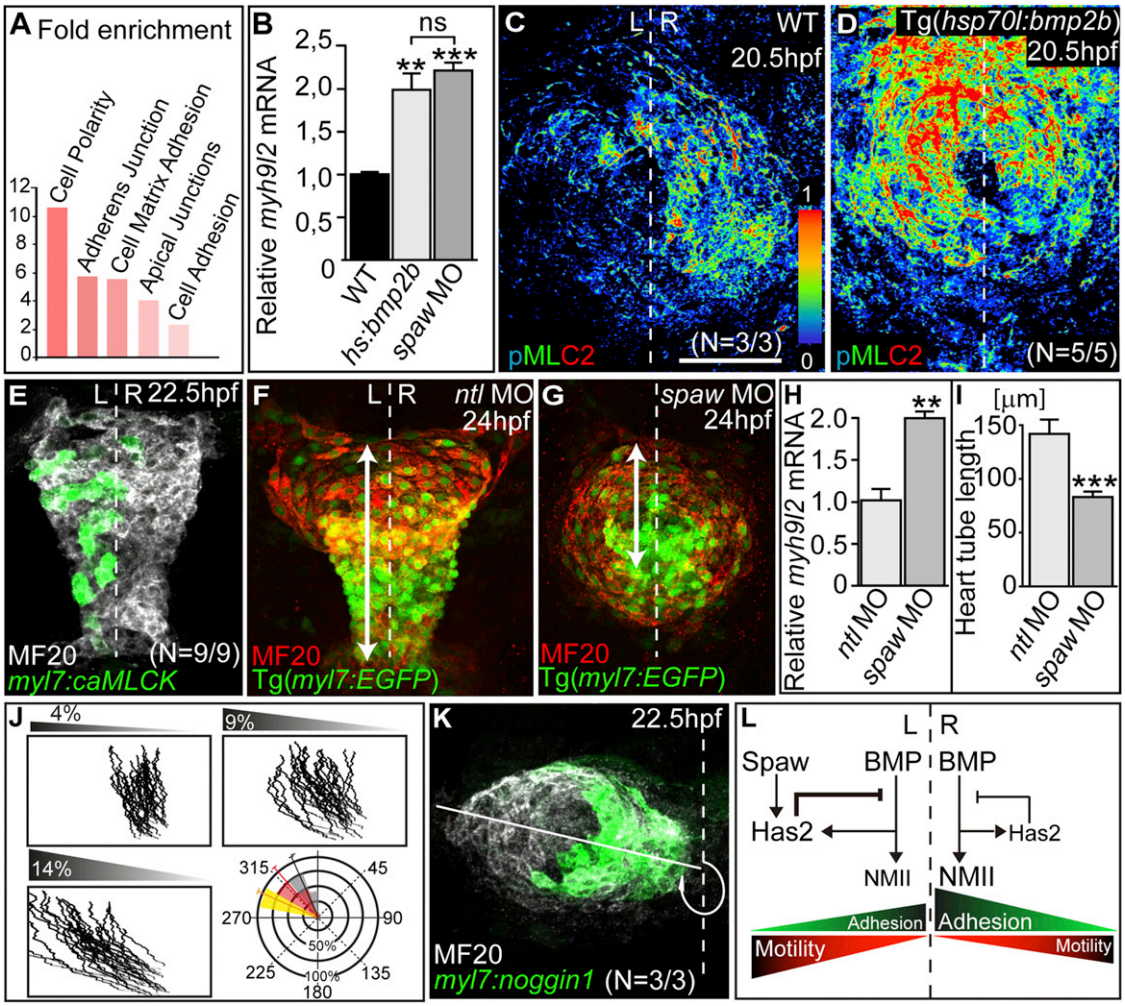

Figure 4. Control of Cardiac Progenitor Cell Motility by Bmp

(A) Enrichment analysis of genes upregulated in Tg[*hsp70l:bmp2b*]^{fr13} versus WT cardiac tissue at 21.5 hpf according to Database for Annotation, Visualization and Integrated Discovery-based clustering for functional terms.

(B) RT-qPCR comparative analysis of relative expression levels of *myh9l2* in cardiac tissue-derived cDNAs at 24 hpf (mean values with SEM; **p < 0.01; ***p < 0.0005).

(C) Expression of phosphorylated NMII (pMLC2) is slightly higher on the right side of the WT cardiac field.

(D) Strong expression of phosphorylated NMII throughout the entire heart cone in Tg[*hsp70l:bmp2b*]^{fr13} transgenic embryos heat shocked at 18 hpf.

(E) Clonal misexpression of caMLCK on the left side of the cardiac cone affects cardiac laterality.

(F and G) Loss of Ntl (F) and Spaw (G) abolishes cardiac laterality, but heart tube elongation is most strongly affected in *spaw* morphants. Heart tube length is the extension between the outflow tract region and leading edge of the atrium (arrows).

(H) RT-qPCR comparative analysis of relative expression levels of *myh9l2* in *spaw* and *ntl* morphant hearts at 24 hpf (mean values with SEM; **p < 0.005).

(I) Heart tube length in *spaw* and *ntl* morphants at 24 hpf (mean values with SEM; ***p < 0.0005).

(J) Simulations of cardiac jogging based on a random cell motility model. Three representative simulations covering a range of L/R differences in cell motility and the respective bearing angles based on ten independent simulations for each condition are shown. The 9% condition of L/R motility differences most closely resembles WT cardiac jogging (red bearing angle).

(K) Clonal misexpression of the Bmp antagonist Noggin1 within the left myocardium enhances the angle of cardiac jogging toward the left.

(L) Model of Nodal-Bmp pathway interactions during stages of cardiac jogging.

Total numbers of embryos indicate the occurrence of the most common phenotypes as shown. L, left; R, right; ns, not significant (for details on statistical analysis, see also Supplemental Experimental Procedures). Scale bars, 50 μm.

See also Figures S3 and S4.

misexpression. As predicted by in silico modeling for an increased L/R bias in cell motility, such myocardial cell clones corresponded with steeper leftward cardiac jogging (Figure 4K; see also Figure S4C). Remarkably, reducing Bmp activity within even small groups of cells impacts the laterality of the entire coherent cardiac tissue, which suggests that individual cell motility rates can affect tissue displacement of larger coherent groups of cells.

DISCUSSION

Our study provides a mechanistic framework for understanding how L/R asymmetric signaling is translated into cellular behavior that generates laterality during heart tube formation. Nodal affects cardiac laterality by asymmetrically upregulating Has2, which, in turn, dampens local Bmp activity (Figure 4L). Reduced Bmp signaling activity on the left determines a L/R bias in NMII levels and causes increased cardiac progenitor cell motility. These findings suggest that molecular L/R asymmetries within the cardiac cone are translated into more-motile versus less-motile states of cardiac progenitor cells on the two contralateral sides. This implies that bilateral differences in cell motility rates are sufficient to confer a high degree of robustness to tissue laterality in a morphogenetic process that produces L/R asymmetries in the heart. The apparent paradox that right-sided cardiac progenitor cells not directly affected by Nodal still respond with leftward motility can be explained by faster motility rates of cardiac progenitor cells on the left generating a pulling force that moves the entire cardiac tissue to the left. Some aspects of cardiac laterality, therefore, may be explained by a random cell motility gradient mechanism that has recently been proposed for chicken axis elongation (Bénazéraf et al., 2010).

The mechanism by which Bmp regulates cell motility may involve NMII, which is activated in an asymmetric L/R pattern in the zebrafish heart cone and in the chicken (Tsuda et al., 1996; Lu et al., 2008) and mouse (Tsuda et al., 1998) looping-stage heart. Here, we show that pharmacological and functional modulations of NMII activity affect cardiac jogging. Similarly, in the *Drosophila* wing disc epithelium, the subcellular distribution of NMII is under direct control of the *Drosophila* Bmp ortholog Decapentaplegic (Dpp) and regulates cuboidal versus columnar cell shapes (Widmann and Dahmann, 2009). Regulation of cardiac progenitor cell shapes within the heart may be one means by which Bmp signaling and NMII activity affect cell motility. Alternatively, NMII may affect cardiac progenitor cells more directly via its well-characterized direct role in cell motility (Conti and Adelstein, 2008).

BMPs are secreted ligands of the TGF-β superfamily with autocrine or paracrine modes of activity during morphogenesis (Umulis et al., 2009). Our work reveals that clonal misexpression of Has2 within myocardial cells reduces Bmp activity, apparently in a cell-autonomous manner, suggesting that hyaluronic acid-proteoglycans affect the autocrine signaling of Bmp ligands. The increased cellular motility associated with the presence of hyaluronic acid may thus be, in part, due to a scavenger function of this ECM component for bioactive Bmp ligands, which would otherwise enhance less-motile properties among cardiac progenitor cells. Has2 is also known to promote cell motility more directly by a cell-intrinsic mechanism that involves activating the small GTPase Rac1 and inducing lamellipodia (Bakkers et al., 2004). In the context of cardiac development, our epistasis experiments reveal that Bmp acts downstream of Has2 in regulating cardiac laterality and that the main effects of Has2 activity during cardiac jogging can be explained by this interaction. Further analyses of the role of ECM composition in conjunction with Bmp signaling may provide mechanistic explanations for a number of cardiac and other developmental defects and diseases that are associated with the ECM (Lockhart et al., 2011; Zhang, 2010).

EXPERIMENTAL PROCEDURES

Expression Constructs and Injections

The Gateway Tol2 kit (Kwan et al., 2007; Villefranc et al., 2007) was used to generate the expression constructs used in this study including *dnbmpr2a* (Monteiro et al., 2008) and *caMLCK* (Blaser et al., 2006). For transient expression, DNA (12.5 ng/μl) was coinjected into one-cell-stage embryos together with transposase mRNA (25 ng/μl). Further details on primers and clones are found in the Supplemental Experimental Procedures. Handling of zebrafish was done in compliance with German and Berlin state law, carefully monitored by the local authority for animal protection (LaGeSo, Berlin-Brandenburg, Germany).

Time-Lapse Imaging and Cell Tracing

Zebrafish embryos were mounted in 1.5% low melting agarose (+0.1% tricaine) covered with E3 medium and imaged at 28.5°C with a 25× objective on a Zeiss LSM 510 META NLO confocal microscope. Time-lapse processing and manual tracking analysis was performed using Volocity (Perkin Elmer, Waltham, MA, USA) and Fiji software (http://fiji.sc/).

Fluorescence Intensity Measurements

Mean plot intensity profiles of indicated heart regions were measured using the Fiji rectangular selection tool subsequently analyzing the plot profile.

Extraction of Tissue and RNA from Heart Samples

Whole hearts were extracted manually from early-stage zebrafish embryos as described elsewhere (Burns and MacRae, 2006). Usually, 150–300 hearts were recovered per isolation. Total RNA was extracted with the RNeasy Micro Kit (QIAGEN) according to the manufacturer's instructions. RNA quality was assessed on a 2100 Bioanalyzer RNA 6000 Nano chip (Agilent Technologies).

Statistical Analysis

Statistical analyses for signal intensity and cell motility measurements were performed using the Student's t test algorithm in Excel (Microsoft).

ACCESSION NUMBERS

The National Center for Biotechnology Information (NCBI) accession number for the microarray data reported in this paper is GSE43888.

SUPPLEMENTAL INFORMATION

Supplemental information includes four figures, four movies, and Supplemental Experimental Procedures and can be found online with this article at http://dx.doi.org/10.1016/j.devcel.2013.01.026.

ACKNOWLEDGMENTS

We thank M. Andrade, J. Bakkers, N. Chi, N. Cornitius, W. Driever, J. Essner, R. Fechner, M.R. Huska, N. Lawson, B. Link, M. Mullins, E. Raz, M. Rebagliati, J. Richter, D.Y. Stainier, U. Strähle, and H.J. Tsai for providing reagents, fish stocks, or other support. We are grateful to Alistair Garratt, Russ Hodge, Francesca Spagnoli, and members of the Abdelilah-Seyfried laboratory for helpful comments on the manuscript. S.A.-S. is supported by a Heisenberg Fellowship of the Deutsche Forschungsgemeinschaft (DFG). This project was supported by Thyssen Grant 10.07.2.128 and DFG Grants SE2016/7-1, NI1167/3-1 ("JIMI"—a network for intravital microscopy), and SFB 815 Project A5.

Received: December 5, 2011
Revised: November 19, 2012
Accepted: January 30, 2013
Published: March 14, 2013

REFERENCES

Amano, M., Ito, M., Kimura, K., Fukata, Y., Chihara, K., Nakano, T., Matsuura, Y., and Kaibuchi, K. (1996). Phosphorylation and activation of myosin by Rho-associated kinase (Rho-kinase). J. Biol. Chem. *271*, 20246–20249.

Baker, K., Holtzman, N.G., and Burdine, R.D. (2008). Direct and indirect roles for Nodal signaling in two axis conversions during asymmetric morphogenesis of the zebrafish heart. Proc. Natl. Acad. Sci. USA *105*, 13924–13929.

Bakkers, J., Kramer, C., Pothof, J., Quaedvlieg, N.E., Spaink, H.P., and Hammerschmidt, M. (2004). Has2 is required upstream of Rac1 to govern dorsal migration of lateral cells during zebrafish gastrulation. Development *131*, 525–537.

Bénazéraf, B., Francois, P., Baker, R.E., Denans, N., Little, C.D., and Pourquié, O. (2010). A random cell motility gradient downstream of FGF controls elongation of an amniote embryo. Nature *466*, 248–252.

Blaser, H., Reichman-Fried, M., Castanon, I., Dumstrei, K., Marlow, F.L., Kawakami, K., Solnica-Krezel, L., Heisenberg, C.P., and Raz, E. (2006). Migration of zebrafish primordial germ cells: a role for myosin contraction and cytoplasmic flow. Dev. Cell *11*, 613–627.

Breckenridge, R.A., Mohun, T.J., and Amaya, E. (2001). A role for BMP signalling in heart looping morphogenesis in Xenopus. Dev. Biol. *232*, 191–203.

Burns, C.G., and MacRae, C.A. (2006). Purification of hearts from zebrafish embryos. BioTechniques *40*, 274–282.

Camenisch, T.D., Spicer, A.P., Brehm-Gibson, T., Biesterfeldt, J., Augustine, M.L., Calabro, A., Jr., Kubalak, S., Klewer, S.E., and McDonald, J.A. (2000). Disruption of hyaluronan synthase-2 abrogates normal cardiac morphogenesis and hyaluronan-mediated transformation of epithelium to mesenchyme. J. Clin. Invest. *106*, 349–360.

Chen, C.M., Norris, D., and Bhattacharya, S. (2010). Transcriptional control of left-right patterning in cardiac development. Pediatr. Cardiol. *31*, 371–377.

Chen, J.N., van Eeden, F.J., Warren, K.S., Chin, A., Nüsslein-Volhard, C., Haffter, P., and Fishman, M.C. (1997). Left-right pattern of cardiac BMP4 may drive asymmetry of the heart in zebrafish. Development *124*, 4373–4382.

Chocron, S., Verhoeven, M.C., Rentzsch, F., Hammerschmidt, M., and Bakkers, J. (2007). Zebrafish Bmp4 regulates left-right asymmetry at two distinct developmental time points. Dev. Biol. *305*, 577–588.

Collery, R.F., and Link, B.A. (2011). Dynamic smad-mediated BMP signaling revealed through transgenic zebrafish. Dev. Dyn. *240*, 712–722.

Conti, M.A., and Adelstein, R.S. (2008). Nonmuscle myosin II moves in new directions. J. Cell Sci. *121*, 11–18.

Dal-Pra, S., Fürthauer, M., Van-Celst, J., Thisse, B., and Thisse, C. (2006). Noggin1 and Follistatin-like2 function redundantly to Chordin to antagonize BMP activity. Dev. Biol. *298*, 514–526.

de Campos-Baptista, M.I., Holtzman, N.G., Yelon, D., and Schier, A.F. (2008). Nodal signaling promotes the speed and directional movement of cardiomyocytes in zebrafish. Dev. Dyn. *237*, 3624–3633.

Jin, S.W., Beis, D., Mitchell, T., Chen, J.N., and Stainier, D.Y. (2005). Cellular and molecular analyses of vascular tube and lumen formation in zebrafish. Development *132*, 5199–5209.

Kwan, K.M., Fujimoto, E., Grabher, C., Mangum, B.D., Hardy, M.E., Campbell, D.S., Parant, J.M., Yost, H.J., Kanki, J.P., and Chien, C.B. (2007). The Tol2kit: a multisite gateway-based construction kit for Tol2 transposon transgenesis constructs. Dev. Dyn. *236*, 3088–3099.

Lawson, N.D., and Weinstein, B.M. (2002). In vivo imaging of embryonic vascular development using transgenic zebrafish. Dev. Biol. *248*, 307–318.

Lecuit, T., Lenne, P.F., and Munro, E. (2011). Force generation, transmission, and integration during cell and tissue morphogenesis. Annu. Rev. Cell Dev. Biol. *27*, 157–184.

Lockhart, M., Wirrig, E., Phelps, A., and Wessels, A. (2011). Extracellular matrix and heart development. Birth Defects Res. A Clin. Mol. Teratol. *91*, 535–550.

Long, S., Ahmad, N., and Rebagliati, M. (2003). The zebrafish nodal-related gene southpaw is required for visceral and diencephalic left-right asymmetry. Development *130*, 2303–2316.

Lu, W., Seeholzer, S.H., Han, M., Arnold, A.S., Serrano, M., Garita, B., Philp, N.J., Farthing, C., Steele, P., Chen, J., and Linask, K.K. (2008). Cellular nonmuscle myosins NMHC-IIA and NMHC-IIB and vertebrate heart looping. Dev. Dyn. *237*, 3577–3590.

Monteiro, R., van Dinther, M., Bakkers, J., Wilkinson, R., Patient, R., ten Dijke, P., and Mummery, C. (2008). Two novel type II receptors mediate BMP signalling and are required to establish left-right asymmetry in zebrafish. Dev. Biol. *315*, 55–71.

Rohr, S., Otten, C., and Abdelilah-Seyfried, S. (2008). Asymmetric involution of the myocardial field drives heart tube formation in zebrafish. Circ. Res. *102*, e12–e19.

Schier, A.F. (2009). Nodal morphogens. Cold Spring Harb. Perspect. Biol. *1*, a003459.

Schilling, T.F., Concordet, J.P., and Ingham, P.W. (1999). Regulation of left-right asymmetries in the zebrafish by Shh and BMP4. Dev. Biol. *210*, 277–287.

Smith, K.A., Chocron, S., von der Hardt, S., de Pater, E., Soufan, A., Bussmann, J., Schulte-Merker, S., Hammerschmidt, M., and Bakkers, J. (2008). Rotation and asymmetric development of the zebrafish heart requires directed migration of cardiac progenitor cells. Dev. Cell *14*, 287–297.

Straight, A.F., Cheung, A., Limouze, J., Chen, I., Westwood, N.J., Sellers, J.R., and Mitchison, T.J. (2003). Dissecting temporal and spatial control of cytokinesis with a myosin II Inhibitor. Science *299*, 1743–1747.

Tsuda, T., Majumder, K., and Linask, K.K. (1998). Differential expression of flectin in the extracellular matrix and left-right asymmetry in mouse embryonic heart during looping stages. Dev. Genet. *23*, 203–214.

Tsuda, T., Philp, N., Zile, M.H., and Linask, K.K. (1996). Left-right asymmetric localization of flectin in the extracellular matrix during heart looping. Dev. Biol. *173*, 39–50.

Umulis, D., O'Connor, M.B., and Blair, S.S. (2009). The extracellular regulation of bone morphogenetic protein signaling. Development *136*, 3715–3728.

Villefranc, J.A., Amigo, J., and Lawson, N.D. (2007). Gateway compatible vectors for analysis of gene function in the zebrafish. Dev. Dyn. *236*, 3077–3087.

Widmann, T.J., and Dahmann, C. (2009). Dpp signaling promotes the cuboidal-to-columnar shape transition of Drosophila wing disc epithelia by regulating Rho1. J. Cell Sci. *122*, 1362–1373.

Zhang, H., and Bradley, A. (1996). Mice deficient for BMP2 are nonviable and have defects in amnion/chorion and cardiac development. Development *122*, 2977–2986.

Zhang, L. (2010). Glycosaminoglycan (GAG) biosynthesis and GAG-binding proteins. Prog. Mol. Biol. Transl. Sci. *93*, 1–17.